Methods for Reducing Leakage Electric Field of a Wireless Power Transfer System for Electric Vehicles

Masaki Jo, Yukiya Sato, Yasuyoshi Kaneko, Shigeru Abe
Graduate School of Science and Engineering
Saitama University
Saitama, Japan
s13mm217@mail.saitama-u.ac.jp

***Abstract*—A wireless power transfer system for electric vehicles has to deal with the issue of high leakage levels of electric field. In this paper, we propose two methods for reducing the leakage electric field. First is the use of ferrite to reduce the emitted leakage electric field to the environment. Second is the changing of the pulse width of the inverter to reduce the harmonics of leakage electric field. We present the experimental results of the reduction effects of leakage electric field. We also compared the leakage electric field using series-parallel and series-series resonant capacitor topologies.**

I. INTRODUCTION

The development and commercialization of electric vehicles (EVs) and plug-in hybrid EVs (PHVs) are actively being pursued because of environmental concerns and increasing oil prices. Current PHVs and EVs require connection to a power supply for battery charging using electric cables. A wireless power transfer system would have numerous advantages: convenient, safe, and maintenance-free. Therefore, wireless power transfer systems are being investigated worldwide [1], [2].

A wireless power transfer system for EVs must have a large air gap and good tolerance to misalignment in the lateral direction. In addition, it must be compact and lightweight. The H-shaped core transformer has been developed to satisfy these requirements [3], [4]. However, it has the issue of leakage electromagnetic field emission from the transformer to the environment. The leakage magnetic and electric fields should be regulated because they may negatively affect the human body and electronic devices. For the effect on the human body, the guideline is defined in the International Commission on Non-Ionizing Radiation Protection (ICNIRP) 2010 [5], and the leakage of the 3-kW H-shaped core transformer should not exceed the reference level at the outside of the vehicle. On the other hand, with regard to the effect on electronic devices, the electric field intensity emitted from an H-shaped core transformer exceeds the reference value set for induction cookers by the Radio Law in Japan. Therefore, the H-shaped core requires some types of countermeasures. However, very few reports concerning the issue of reducing leakage electric field are available.

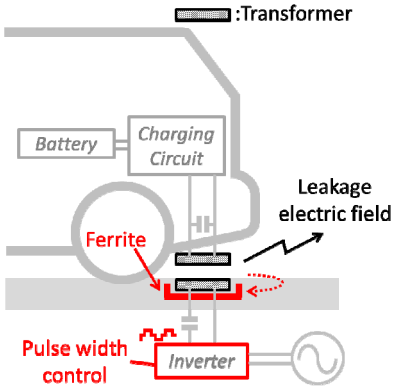

Figure 1. Methods for reducing the leakage electric field.

In this paper, we propose two methods for reducing the leakage electric field intensity (Fig. 1). Here, the leakage electric field is defined as the equivalent electric field, which is calculated as $E = Z \times H$, where E is the electric field, H is the measured magnetic field, and Z is the impedance in free-space (120 π). Therefore, reducing the magnetic field is necessary to reduce the equivalent electric field. The first method uses ferrite to reduce the propagation of the leakage electric field. The second method employs pulse width control of the inverter to reduce the harmonic current at the primary side and the leakage electric field. We compared the primary magnetomotive force with the secondary one and showed that reducing the harmonic current at the primary side is more effective. We confirmed the effectiveness of both methods by an experiment that measured the leakage electric field intensity. We also compared the leakage electric field using series-parallel (SP) and series-series (SS) resonant capacitor topologies.

978-1-4799-5776-7/14/$31.00 ©2014 IEEE

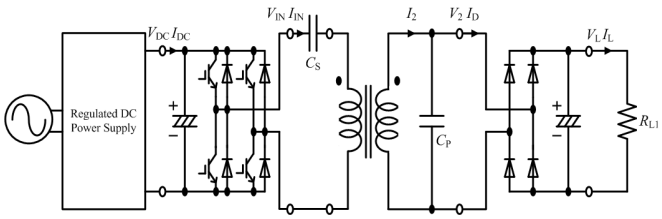

Figure 2. Wireless power transfer system.

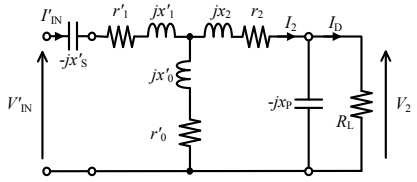

Figure 3. Detailed equivalent circuit.

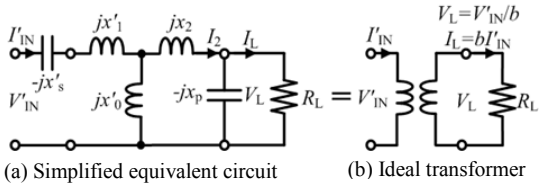

(a) Simplified equivalent circuit (b) Ideal transformer

Figure 4. (a) Simplified equivalent circuit. (b) Ideal transformer.

II. Primary and Secondary Currents of a Transformer

The equivalent leakage electric field depends on the magnetomotive force *NI*, which is the product of the number of turns *N* and the winding current *I* in a wireless power transfer system. Therefore, examining the magnitude and phase angle of primary current I_{IN} and secondary current I_2 is important. Fig. 2 shows a schematic diagram of the contactless power transfer system using series and parallel resonant capacitors. A full-bridge inverter is used as a high-frequency power supply.

Fig. 3 shows the detailed equivalent circuit, which consists of a T-shaped equivalent circuit with resonant capacitors C_S and C_P and load resistance R_L. The primary values are converted into equivalent secondary values using the turn ratio $a = N_1/N_2$. Because the winding resistances and ferrite-core loss are considerably lower than the leakage and mutual reactances at the resonant frequency, the winding resistances (r'_1 and r'_2) and ferrite-core loss r'_0 can be ignored (Fig. 4 (a)).

The secondary parallel capacitor C_P and the primary series capacitor C_S can be expressed as

$$\frac{1}{\omega_0 C_P} = x_P = \omega_0 L_2 = x'_0 + x_2 ,$$

$$\frac{1}{\omega_0 C'_S} = x'_s = \frac{x'_0 x_2}{x'_0 + x_2} + x'_1 . \qquad (1)$$

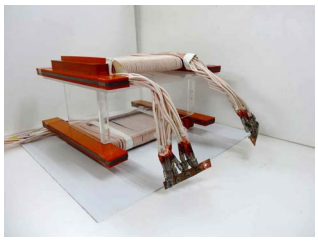

Figure 5. Outline of an H-shaped transformer.

TABLE I. Transformer Specifications

Type		H-shaped core
Weight[kg]	Primary	6.70
	Secondary	6.43
Winding	Primary	3p×20T
	Secondary	15p×4T

TABLE II. Transformer Parameters

Type	H-shaped core
f_0 [kHz]	50
r_1 [mΩ]	136
r_2 [mΩ]	5.25
l_0 [μH]	28.4
l_1 [μH]	117
l_2 [μH]	4.87
C_S [μF]	0.0722
C_P [μF]	1.70
k	0.192
b	0.189
R_{Lmax} [Ω]	10.3
η_{max} [%]	97.0

The input voltage V'_{IN} and the input current I'_{IN} can be expressed as

$$V'_{IN} = \frac{V_{IN}}{a} = b V_2 , \quad I'_{IN} = aI_{IN} = \frac{I_L}{b} , \quad b = \frac{x'_0}{x'_0 + x_2} . \qquad (2)$$

Equation (2) shows that the equivalent circuit of a transformer with these capacitors is the same as that of an ideal transformer with turn ratio *b* at the resonant frequency (Fig. 4 (b)).

The relationship between I_{IN} and I_2 can be expressed as

$$I_2 = \left(1 - \frac{x'_S - x'_1}{x'_0} + j\frac{Z'}{x'_0}\right) I'_{IN} = acI_{IN}$$

$$\left(c = 1 - \frac{x'_S - x'_1}{x'_0} + j\frac{Z'}{x'_0}\right). \qquad (3)$$

where Z' is $\{x'_0/(x'_0+x_2)\}^2$. From (3), we can determine whether I_{IN} or I_2 causes more leakage electric field.

III. Leakage Electromagnetic Field in an H-shaped Core Transformer

A. Transformer Specifications

The leakage magnetic and electric fields should be regulated because they may negatively affect the human body and electronic devices. ICNIRP provides the reference levels for human body, and the Radio Law in Japan provides the reference levels for electronic devices. In this section, we compare the electromagnetic field with the specified reference levels and investigate the necessity of decreasing the electromagnetic field. The specifications of the transformer used in our experiment are shown in Fig. 5 and Table I and II.

B. Leakage Magnetic Field

The leakage magnetic flux may negatively affect the human body. The reference level of the leakage flux density (27 μT at 50 kHz) is set by ICNIRP 2010. Fig. 6 shows the leakage flux density of the H-shaped core transformer with a mechanical gap length of 150 mm without misalignment and with a 3-kW output power. Owing to the directionality of the H-shaped core transformer, the measurement is performed in the forward direction x and lateral direction y. The decrease of flux density in the x direction can be expressed as $B \propto r^{-2.7}$, whereas that in the y direction can be expressed as $B \propto r^{-2.5}$, (B is the flux density, and r is distance from the center of the transformer).

The leakage flux densities of the H-shaped core transformer in the x and y directions are below 27 μT at distances of 650 and 500 mm from the center of the transformer, respectively. Thus, the H-shaped core transformer can be considered safe from outside a vehicle if the vehicle width is 1700 mm and the transformer is attached to the vehicle center.

C. Leakage Electric Field

The leakage electric field may negatively affect electronic devices. Because no clear standard of leakage electric field is currently set for wireless power transfer system for EVs, we examined the leakage electric field using the criteria for induction cookers as a reference, which is defined by Article 46-7 of the Enforcement Regulations of the Radio Law in Japan (JP-46-IH). The reference level is determined for a distance of 30 m, and because our measurement was at 3 m, we converted the reference level to the 3-m value (106 dB μV/m, except for the operating frequency). The measurement of the electric field intensity was performed under the following conditions: 1.5 kW, 50 kHz, mechanical gap length of 150 mm with no misalignment, and distance of 3 m in a fully anechoic room. A 60-cm-diameter loop antenna (ETS-Lindgren Model 6512) was used in the measurement.

Fig. 7 and Table III show the leakage electric field intensity of the H-shaped core transformer. Compared with the criteria for induction cookers, the electric field intensities of the H-shaped core transformer are approximately 26, 14, and 3 dB over the criteria at 50, 150, and 250 kHz, respectively. Thus, reducing the electric field intensity in the H-shaped core transformer is important.

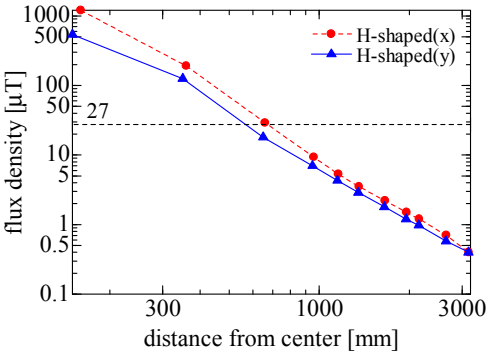

Figure 6. Flux density (P_{OUT} = 3 kW).

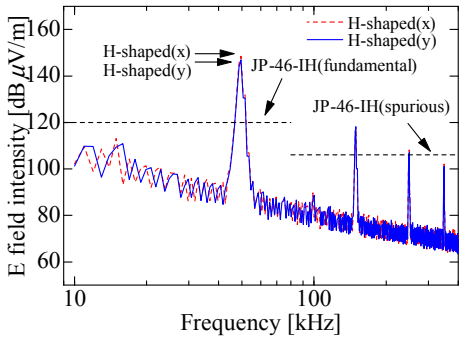

Figure 7. Electric field intensity (P_{OUT} = 1.5 kW).

IV. Method for Reducing the Leakage Electric Field

Two methods are available to reduce the leakage electric field. One is to control the propagation path of the leakage electric field by shielding the electromagnetic waves emitted from the transformer. The other is to control the generation source of the leakage electric field by reducing the harmonic current flowing in the transformer.

The former method investigates the reduction effect of the leakage electric field using a ferrite shield placed at the back of an aluminum sheet. The latter method investigates the harmonic reduction effect of the leakage electric field using pulse width control inverter.

A. Propagation Path Control

1) Reduction effect of ferrite shield

To reduce the leakage electric field externally radiated from the transformer, we propose a method that uses a ferrite with a high magnetic permeability at the back of an aluminum sheet. Fig. 8 shows the sizes of the ferrite and the aluminum sheet. Considering the weight of the onboard-side device, the ferrite shield is used only at the primary side. The experimental conditions are the same as those described in the previous section.

TABLE III. ELECTRIC FIELD INTENSITY USING FERRITE SHIELD

Type		P_{OUT} [kW]	Al sheet [mm]	Electric field intensity [dB μV/m]			
				50 kHz	150 kHz	250 kHz	350 kHz
Before countermeasures	H-shaped	1.5	450 × 450	146.2	119.6	108.9	103.2
Propagation path control	Plate + Frame	1.5	450 × 450	143.3	113.3	100.6	94.6
		1.5	600 × 600	142.0	112.4	100.9	95.5
	Plate	1.5	600 × 600	143.4	114.8	103.4	97.5
	Frame	1.5	600 × 600	144.2	116.2	104.5	99.1
JP-46-IH (3m)		-	-	120	106	106	106

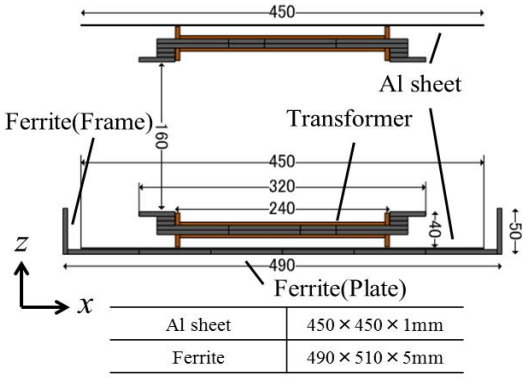

Figure 8. Dimensions of the transformer and ferrite shield.

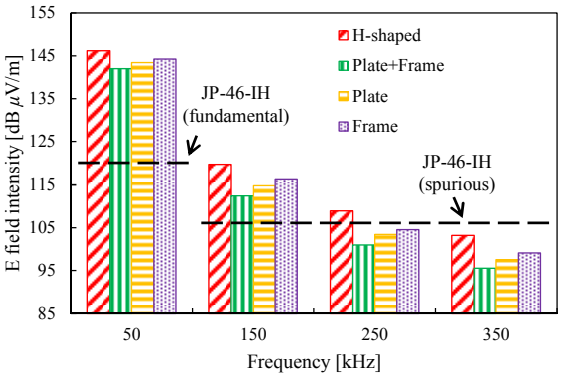

Figure 10. Electric field intensity using ferrite shield.

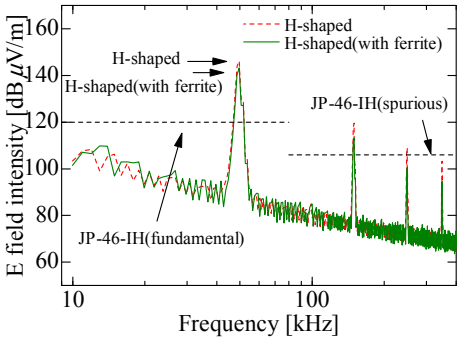

Figure 9. Electric field intensity using ferrite shield.

Fig. 9 and Table III show the measurement result of the leakage electric field intensity. The leakage electric field intensity with the ferrite shield was lower than that without it. The electric field intensity was reduced by approximately 2.9, 6.3, 8.4, and 8.6 dB at 50, 150, 250, and 350 kHz, respectively. However, the coupling factor k decreased from 0.192 to 0.135, and the transformer efficiency decreased from 93.1% to 90.1%.

2) Improvement in efficiency

The main flux was reduced because the magnetic flux generated by the primary side was not coupled to the secondary side but to the ferrite shield since the distance between the ferrite shield and the magnetic poles of the primary transformer was close. Therefore, the transformer efficiency was reduced when the ferrite shield was used. To solve this problem, we considered increasing the size of the aluminum sheet to increase the distance between the ferrite shield and the magnetic poles. By changing the aluminum sheet size from 450 mm × 450 mm to 600 mm × 600 mm and the ferrite shield size from 490 mm × 510 mm to 650 mm × 660 mm, the coupling factor k increased from 0.135 to 0.165.

Fig. 10 and Table III show the measurement result of the leakage electric field intensity. The electric field intensity was reduced by approximately 7.2, 8.1 and 7.7 dB at 150, 250 and 350 kHz, respectively. The reduction effect was almost the same as that of the 490 mm × 510 mm ferrite shield, and the transformer efficiency improved from 90.1% to 92.7%.

3) Ferrite amount reduction

The use of ferrite for shielding has become increasingly costly. To reduce ferrite usage, we studied the leakage electric field in cases where only a ferrite plate and only a ferrite frame are individually used. Fig. 10 and Table III show the measurement result of the leakage electric field intensity. Compared with that without any countermeasure, the leakage electric field intensity with only the ferrite plate was reduced by approximately 4.8, 5.6, and 5.7 dB at 150, 250, and 350 kHz, respectively. That with only the ferrite frame was respectively reduced by approximately 3.4, 4.5, and 4.2 dB. The reduction effects in both cases were lower than those when the plate and frame were used together.

By performing magnetic field analysis of the ferrite shield using JMAG software, we found that the magnetic flux density of the ferrite at the back of the aluminum plate is

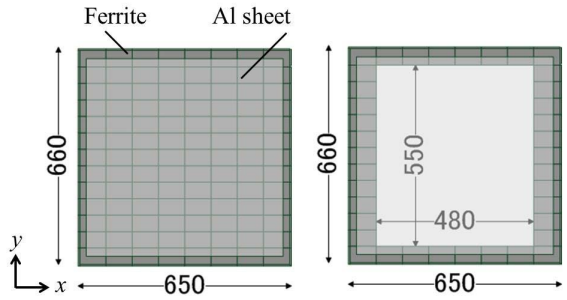

(a) Plate + frame (b) Reduction in the ferrite

Figure 11. Reduction in the ferrite amount.

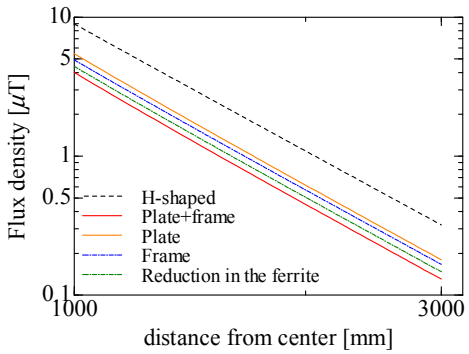

Figure 12. Flux density (reduction in the ferrite).

relatively low. Therefore, we performed the analysis for the case where the ferrite amount in the x–y plane was reduced by approximately 62%, as shown in Fig. 11(b). Fig. 12 shows the simulated result of the magnetic flux density 3 m from the center of the transformer. The magnetic flux density for the case of the ferrite with a 62% reduction was lower than those when only the ferrite plate and only the ferrite flame models were individually used. The reduction effect of the magnetic flux density for the case of the ferrite with a 62% reduction was similar to that when the frame and plate were combined. From these results, we can possibly reduce the ferrite amount by approximately 62% despite a slight decrease in the effect.

B. Generation Source Control

1) Comparison of magnetomotive forces

The equivalent leakage electric field intensity is proportional to the magnetomotive force NI. The transformer is divided into the ground-side primary coil and onboard-side secondary coil, and we do not know which side has more effect on the leakage electric field. This section first presents which side, whether the primary or the secondary side can be effectively controlled for the generation source by calculating and comparing the primary and secondary magnetomotive forces N_1I_{IN} and N_2I_2.

The relationship between I_{IN} and I_2 is expressed by (3). Because $a = N_1/N_2$, the relationship between N_1I_{IN} and N_2I_2 is given by

$$N_2I_2 = cN_1I_{IN}\,. \tag{4}$$

Because the reactances of capacitors C_S and C_P in terms of the harmonics are small, the relationship between N_1I_{IN} and N_2I_2 is approximately given by

$$N_2I_2 \approx bN_1I_{IN}\,. \tag{5}$$

The c values in (3) at 50, 150, 250, and 350 kHz were calculated as 1.1 0.22, 0.20, and 0.19, respectively. Substituting the values of c in (4) yielded approximately the same primary and secondary magnetomotive forces at an operating frequency of 50 kHz. However, the primary magnetomotive force was approximately five times larger than the secondary one at 150 kHz or higher. Hence, primary-side control of the generation source is more effective than secondary-side control. Thus, we used a pulse width control inverter for the primary-side harmonic current reduction.

2) Primary-side generation control

When a square-wave inverter is used as a high-frequency power supply, the input voltage has a harmonic component

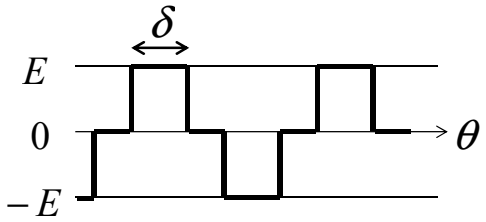

Figure 13. Pulse width control inverter.

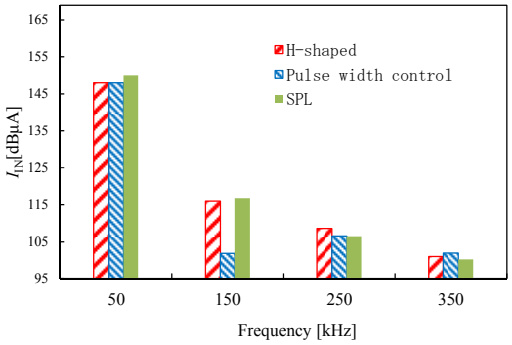

(a) Primary winding

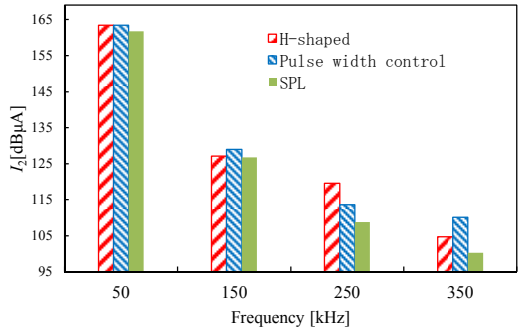

(b) Secondary winding

Figure 14. Harmonic currents.

TABLE IV. ELECTRIC FIELD INTENSITY WITH GENERATION SOURCE CONTROL

Type		P_{OUT} [kW]	Al sheet [mm]	E field intensity [dB μV/m]			
				50 kHz	150 kHz	250 kHz-	350 kHz
Before countermeasures	H-shaped	1.0	450 × 450	146.0	117.1	107.0	101.5
		1.5	450 × 450	146.2	119.6	108.9	103.2
Generation source control	Pulse width control	1.0	450 × 450	145.9	107.6	107.3	98.1
	SPL	1.5	450 × 450	145.1	119.7	108.4	102.0
Propagation path and generation source control	Ferrite shield and pulse width control	1.0	600 × 600	141.6	88.5	100.4	90.6
JP-46-IH (3m)		-	-	120	106	106	106

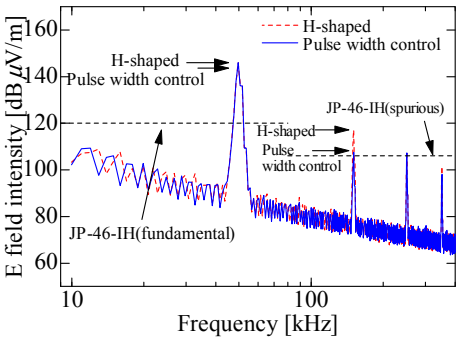

Figure 15. Electric field intensity (Pulse width control).

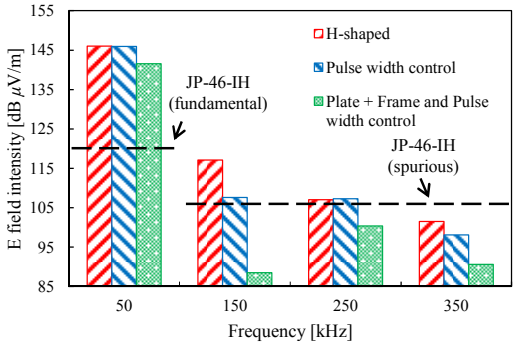

Figure 16. Electric field intensity.

whose magnitude is inversely proportional to the order. For this reason, the primary current includes the harmonics. We adopted a pulse width control inverter. Fig. 13 shows the pulse width control wave-form. Pulse width δ was set to a value that can reduce the leakage electric field at the third harmonic of 150 kHz.

Fig. 14 shows the simulated result of harmonic currents I_{IN} and I_2. I_{IN} was reduced by approximately 15 dB at 150 kHz. Figs. 15 and 16 and Table IV show the measurement results of the leakage electric field intensity. The experimental conditions were the same as those described in Section 3 except that the output power was 1.0 kW. The electric field intensity under the pulse width control became approximately −9.6, +0.3, and −3.3 dB at 150, 250, and 350 kHz, respectively, compared with that without the control.

3) Secondary-side generation control

To verify that the effect of the secondary-side generation control is small, the experiment was performed using an SPL topology that inserted reactor L_S before the full-wave rectifier [4].

When a full-wave rectifier is used, the current that flows through the rectifier has a pulsed waveform that flows only around the peak of the rectifier input voltage. Therefore, I_2 includes the harmonics. The use of the SPL topology can suppress the harmonic current that flows to the rectifier circuit and can reduce the harmonic component of I_2.

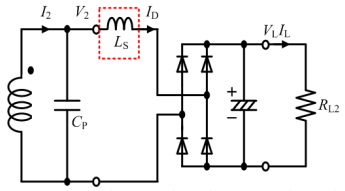

Figure 17. L inserted at the secondary side.

Fig. 17 shows the schematic diagram of the SPL topology. L_S is determined to have the same value as L_2, as shown in (6).

$$\omega_0 L_S = \omega_0 L_2 = x_0' + x_2 \tag{6}$$

Fig. 14 shows the simulated result of harmonic currents I_{IN} and I_2. I_2 was reduced by approximately 11 and 14 dB at 250 and 350 kHz, respectively.

Table IV shows the measurement results of the leakage electric field intensity of the SPL topology when the output power is 1.5 kW. The electric field intensity using the SPL topology became approximately +0.1, −0.5, and −1.2 dB at 150, 250, and 350 kHz, respectively. The reduction effect of the SPL topology was low, although the harmonic component of I_2 was reduced.

4) Pulse width control using ferrite shield

By combining the two methods, i.e., when the ferrite shield and pulse width control of the inverter were used, the electric field intensity was reduced by 4.6, 28.6, 6.6, and 10.9 dB at 50, 150, 250, and 350 kHz, respectively (Fig. 16 and Table IV).

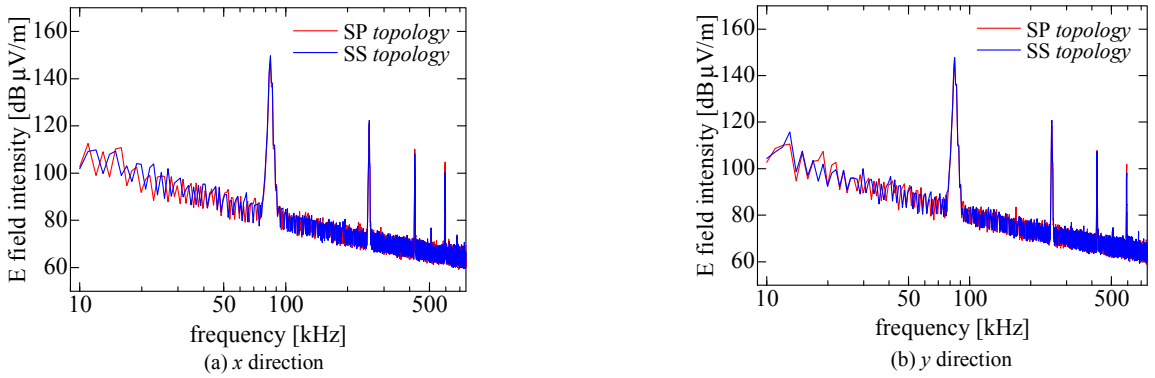

Figure 19. Electric field intensity of the SP and SS topologies.

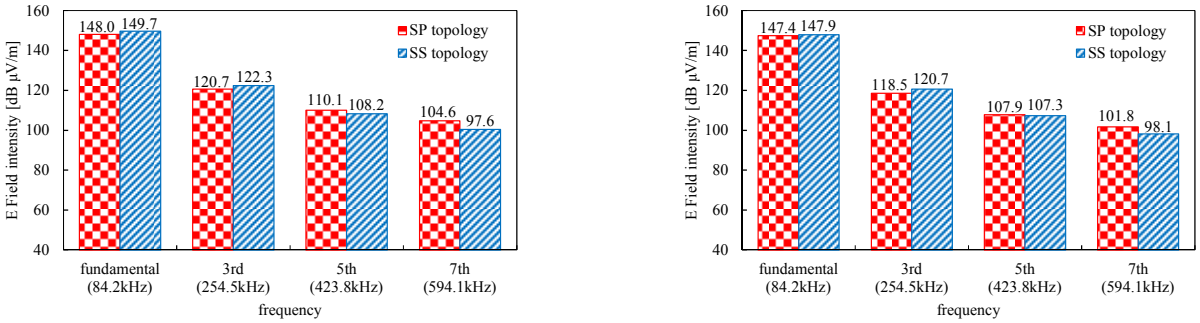

Figure 20. Comparison of electric field intensity of fundamental and harmonic components.

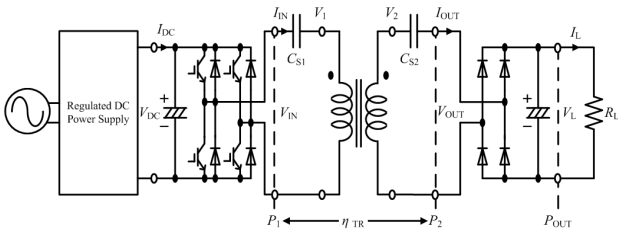

Figure 18. Schematic diagram of the SS topology.

From these results, we confirmed that the proposed methods are effective in reducing the leakage electric field intensity.

V. Leakage Electric Field Intensity of the SP and SS Topologies

The SP and SS topologies are the most common capacitor compensation topologies. In this section, we compare the SP and SS topologies when the operating frequency is 85 kHz and the output power is 3 kW. Fig. 18 shows the schematic diagram of the SS topology. The primary series capacitor C_{S1} and secondary series capacitor C_{S2} values that resonate with each self-inductance value are determined as follows:

$$\frac{1}{\omega_0 C'_{S1}} = x'_{s1} = x'_0 + x'_1 , \quad \frac{1}{\omega_0 C_{S2}} = x_{s2} = x'_0 + x_2 . \tag{7}$$

TABLE V. Transformer Parameters

Type	SP topology	SS topology
Winding	4p×14T	
	15p×4T	4p×14T
f_0 [kHz]	85	
r_1 [mΩ]	85.8	81.7
r_2 [mΩ]	7.55	77.4
l_0 [μH]	13.7	14.3
l_1 [μH]	58.4	57.3
l_2 [μH]	4.62	56.5
C_S [μF]	0.0504	0.0491
C_P [μF]	0.611	0.0497
k	0.192	0.199
R_{Lmax} [Ω]	15.5	7.3
η_{max} [%]	97.4	97.9

Table V lists transformer parameters of the SP and SS topologies. Figs. 19 and 20 show the leakage electric field intensity in the x and y directions. The leakage electric field intensity is proportional to the sum of the primary and the secondary magnetomotive forces. From the experimental results, the magnetomotive force of the SP topology was 368 A, and that of the SS topology was 399 A. The

magnetomotive forces were approximately the same, and the leakage electric field intensity was at the same level.

VI. CONCLUSION

The H-shaped core transformer for wireless power transfer system has to deal with the issue of high levels of leakage electric field intensity. We have proposed two methods for reducing the leakage electric field intensity using ferrite as a propagation path control and pulse width control of the inverter as a generation source control. When the ferrite was used, the leakage electric field intensity was reduced by approximately 2.9, 6.3, 8.4, and 8.6 dB at 50, 150, 250, and 350 kHz, respectively. When the pulse width control of the inverter was used, the leakage electric field intensity at 150 kHz was reduced to approximately 9.6 dB. A further countermeasure against the leakage electric field at an operating frequency of 50 kHz is necessary. We also confirmed that the leakage electric field intensity of the SP and SS topologies are at the same leakage level.

REFERENCES

[1] M. Budhia, G. A. Covic, and J. T. Boys, "A new IPT magnetic coupler for electric vehicle charging systems," IEEE IECON 2010, pp. 2481–2486, 2010.

[2] M. Budhia, G. A. Covic, J. T. Boys and C. Y. Huang, "Development and evaluation of a single sided magnetic flux coupler for contactless electric vehicle charging," in proceedings of IEEE ECCE 2011, pp. 614–621, 2011.

[3] M. Chigira, Y. Nagatsuka, Y. Kaneko, S. Abe, T. Yasuda, and A. Suzuki, "Small-size light-weight transformer with new core structure for contactless electric vehicle power transfer system," ECCE2011-PHOENIX, pp. 260–266, 2011.

[4] H. Takanashi, Y. Sato, Y. Kaneko, S. Abe, and T. Yasuda, "A large air gap 3 kW wireless power transfer system for electric vehicles," ECCE2012, North Carolina, pp. 269–274, 2012.

[5] International Commission on Non-Ionizing Radiation Protection (ICNIRP), "Guidelines for limiting exposure to time varying electric, magnetic, and electromagnetic fields," 2010.

[6] Soichiro Nakadachi, Shigeru Mochizuki, Sho Sakaino, Yasuyoshi Kaneko, Shigeru Abe, Tomio Yasuda, "Bidirectional contactless power transfer system expandable from unidirectional system", ECCE2013, Denver, pp. 505, 2013.